

## Expression patterns of tight junction proteins in porcine major salivary glands: a comparison study with human and murine glands

Xue-Ming Zhang,<sup>1</sup>  Yan Huang,<sup>1</sup> Kuo Zhang,<sup>3</sup> Ling-Han Qu,<sup>1</sup> Xin Cong,<sup>2</sup> Jia-Zeng Su,<sup>1</sup> Li-Ling Wu,<sup>2</sup> Guang-Yan Yu<sup>1\*</sup> and Yan Zhang<sup>2</sup>

<sup>1</sup>Center for Salivary Gland Diseases, Department of Oral and Maxillofacial Surgery, Peking University School and Hospital of Stomatology, Beijing, China

<sup>2</sup>Department of Physiology and Pathophysiology, Key Laboratory of Molecular Cardiovascular Sciences, Ministry of Education and Beijing Key Laboratory of Cardiovascular Receptors Research, Peking University School of Basic Medical Sciences, Beijing, China

<sup>3</sup>Department of Laboratory Animal Science, Peking University Health Science Center, Beijing, China

### Abstract

Tight junction (TJ) proteins play a dynamic role in paracellular fluid transport in salivary gland epithelia. Most TJ studies are carried out in mice and rats. However, the morphology of rodent salivary glands differs from that of human glands. This study aimed to compare the histological features and the expression pattern of TJ proteins in porcine salivary glands with those of human and mouse. The results showed that porcine parotid glands were pure serous glands. Submandibular glands (SMGs) were serous acinar cell-predominated mixed glands, whereas sublingual glands were mucous acinar cell-predominated. Human SMGs were mixed glands containing fewer mucous cells than porcine SMGs, whereas the acinar cells of murine SMGs are seromucous. The histological features of the duct system in the porcine and human SMGs were similar and included intercalated, striated and excretory ducts, but the murine SMG contained a specific structure, the granular convoluted tubule. TJ proteins, including claudin-1 to claudin-12, occludin and zonula occludin-1 (ZO-1), were detected in the porcine major salivary glands and human SMGs by RT-PCR; however, claudin-6, claudin-9 and claudin-11 were not detected in the murine SMG. As shown by immunofluorescence, claudin-1, claudin-3, claudin-4, occludin and ZO-1 were distributed in both acinar and ductal cells in the porcine and human SMGs, whereas claudin-1 and claudin-3 were mainly present in acinar cells, and claudin-4 was mainly distributed in ductal cells in the murine SMG. In addition, 3D images showed that the TJ proteins arranged in a honeycomb-like structure on the luminal surface of the ducts, whereas their arrangements in acini were irregular in porcine SMGs. In summary, the expression pattern of TJ proteins in salivary glands is similar between human and miniature pig, which may be a candidate animal for studies on salivary gland TJ function.

**Key words:** miniature pig; mucous acinus; salivary gland; serous acinus; tight junction.

### Introduction

Salivary glands consist of three pairs of major salivary glands, the parotid glands (PGs), submandibular glands

(SMGs) and sublingual glands (SLGs), as well as numerous minor salivary glands located within the lamina propria throughout oral mucosa. The major salivary glands secrete 90% of saliva in human (Pedersen et al. 2002). Primary saliva is formed by salivary epithelia through transcellular and paracellular pathways. Tight junctions (TJs) form the primary barrier against the paracellular diffusion of solutes, thus maintaining the selective transepithelial ion gradients needed for salivary secretion (Anderson, 2001; Miyoshi & Takai, 2005, 2008; Mineta et al. 2011). TJ proteins are transmembrane proteins, including claudins, occludin, junctional adhesion molecules, and the family of zonula occludin (ZO) proteins, which anchor TJ transmembrane proteins to the actin cytoskeleton. TJ proteins are quite complex and diverse in function. For instance, the claudin superfamily

#### Correspondence

Yan Zhang, Department of Physiology and Pathophysiology, Peking University School of Basic Medical Sciences, Beijing 100191, China.  
T: + 86 010 82802403; F: + 86 010 82802403; E: zhangy18@bjmu.edu.cn  
and

Guang-Yan Yu, Department of Oral and Maxillofacial Surgery, Peking University School and Hospital of Stomatology, Beijing 100081, China.  
T: + 86 010 82195245;

E: + 86 010 62173402; E: gyyu@263.net

Accepted for publication 30 April 2018

Article published online 31 May 2018

has expanded to 27 members in human and mouse (Mineta et al. 2011). Among them, claudin-2 and claudin-4 are linked to intercellular  $\text{Na}^+/\text{K}^+$  permeability (Van Itallie et al. 2001; Amasheh et al. 2002), and claudin-16 is essential for  $\text{Ca}^{2+}/\text{Mg}^{2+}$  resorption (Simon et al. 1999; Muller et al. 2003), suggesting that individual claudins mediate specific functions. Several studies have shown that TJ proteins play a dynamic role in paracellular fluid secretion in the salivary gland epithelium and that the expression and organization are altered during several pathological processes, such as Sjogren's syndrome (SS; Mellas et al. 2015). ZO-1 and occludin are downregulated, whereas claudin-1 and claudin-4 are upregulated and redistributed from the apical to the basolateral side of acinar cells in minor salivary glands from SS patients (Ewert et al. 2010). Limited observation of post-irradiated human SMGs also shows a loss of ZO-1 staining (Li et al. 2005). The alteration of the TJ expression and organization in salivary glands with SS and radiation-induced xerostomia suggests that these proteins might play important roles in the process of salivary gland dysfunction. However, the specific role of individual proteins under physiological or pathological circumstances is still not well understood. Rodents, which are easy to manipulate, are widely used in studies on salivary glands, but limitations exist when the proven strategies for disease prevention and treatment are translated into clinical use because of the differing anatomical, histological and biochemical characteristics between rodents and human. The salivary glands of the miniature pig are considered much more similar to those of humans in terms of anatomical and histological structures and are increasingly accepted in salivary gland studies, including studies of irradiation injury, gene transfer, functional reconstruction, and development (Zhou et al. 2010; Guo et al. 2014; Wang et al. 2015; Nam et al. 2016; Zhu et al. 2016). However, the expression pattern of TJ proteins in porcine salivary glands has not been investigated so far. Thus, this study aims to compare the histological features and expression pattern of the TJ proteins in the porcine major salivary glands with those of human and mouse and to evaluate using the miniature pig as an animal model in studies on salivary glands.

## Materials and methods

### Tissue preparation

The use of human and animal tissue was approved by the Ethics Committee for Human Experiments of Peking University and the Ethics Committee of Animal Research, Peking University Health Science Center, and was in accordance with the ARRIVE guidelines (NC3Rs Reporting Guidelines Working Group, 2010). Ten human SMGs were collected during functional neck dissection for primary tongue squamous carcinoma and were histologically confirmed normal by a pathologist. Ten healthy male Bama miniature pigs (8–10 months old) and 10 male C57BL/6J (8 weeks old)

mice were included in this study. The major salivary glands were collected from the miniature pigs under general anesthesia with Zoletil (20 mg  $\text{kg}^{-1}$ ) and 3–5% isoflurane via mask induction. The mice were anesthetized with ether and sacrificed by cervical dislocation, and the SMGs were removed and used for the following studies.

### Regents and antibodies

Alcian Blue 8GX was purchased from Sigma-Aldrich (St. Louis, MO, USA). Primary antibodies against claudin-1 (BS1063), claudin-3 (BS1067), claudin-4 (BS1068) and claudin-7 (BS1070) were from Bio-world Technology (Minneapolis, MN, USA). Primary antibodies against occludin (71-1500), ZO-1 (40-2200) and Alexa-Fluor-488- and Alexa-Fluor-594-conjugated secondary antibodies were from Thermo Fisher Scientific (Beverly, MA, USA).

### Histochemical staining

Tissues were fixed in 4% paraformaldehyde, embedded in paraffin wax and cut into serial sections of 5  $\mu\text{m}$ . Adjacent sections were processed for routine staining by Hematoxylin and eosin (H&E). For determining the components of the secretory granules, the sections were immersed in 1% Alcian Blue (pH 2.5) for 15 min and oxidized in 1% periodic acid solution for 10 min. After rinsing, the sections were immersed in Schiff's reagent for 15 min and counterstained with hematoxylin. Images of the gland parenchyma were randomly obtained from six views of three sections of each gland and captured under a light microscope (Q550CW, Leica, Manheim, Germany). The area of the serous or mucous cells was quantified using IMAGEJ software (National Institutes of Health, Bethesda, MD, USA). The relative area of serous acinar cells to the whole acinar area was calculated. The results are presented as the means  $\pm$  SEM, and an unpaired Student's *t*-test was used to compare the differences between human and porcine SMGs. A *P*-value of  $< 0.05$  was considered statistically significant.

### Immunofluorescence

Tissues were fixed in 4% paraformaldehyde, dehydrated in 30% sucrose and embedded in OCT (optimal cutting temperature compound). Sections of 15  $\mu\text{m}$  were cut in a cryostat. The sections were immersed in citrate buffer (pH 6.0) and heated in a microwave oven for antigen retrieval. After being blocked with 5% bovine serum albumin, the sections were incubated at 4 °C overnight with the primary antibodies diluted 1 : 100 or 1 : 200 in phosphate-buffered saline (PBS). Then, the sections were incubated with secondary antibody at 37 °C for 1 h. Nuclei were stained with 4',6-diamidino-2-phenylindole (DAPI). Confocal images were captured by a laser scanning confocal microscope (Leica TCS SP8, Wetzlar, Germany). The 3D images were recreated using IMARIS 3D/4D image visualization and analysis software (Bitplane AG, Zurich, Switzerland; version 7.2.3).

### Transmission electron microscopy

Tissues were fixed in 2% glutaraldehyde and postfixed in 1% osmium tetroxide. Ultrathin sections were produced, stained with 10% uranyl acetate and 1% lead citrate, and examined with a transmission electron microscope (HITACHI H-7000, Tokyo, Japan).

**Table 1** Primers for porcine tight junction component mRNA.

Gene	Forward primer (5'-3')	Reverse primer (5'-3')	Size (bp)
<i>Sus scrofa</i> (pig)			
<i>Cldn1</i>	AAGATTTACTCCTACGCTGGT	CTTGGTGTGGTAAGATG	141
<i>Cldn2</i>	CAT CCT CTG CTT TCTG	AACTCACTCTGGCTTG	126
<i>Cldn3</i>	AAGCCAAGATCCTACTCC	G TAGTCCTCGGGTCGTA	83
<i>Cldn4</i>	CCTTCATCGGCAGCAACA	GCAGCGAGTCGTACACCTG	111
<i>Cldn5</i>	ACTTGAAGGGCTGTGGAT	GGCACAGTCGGTCGTAGAA	323
<i>Cldn6</i>	TGGTCCAGCTCAGGGTAGG	ACACGCCATATCAGGACTT	303
<i>Cldn7</i>	AGGCATCATTTATCGT	GACAAGAGCAAGAGAGCAG	194
<i>Cldn8</i>	TGCTTGGTGGTGTGGAATG	TGCAAGTTCATCCACAGTC	129
<i>Cldn9</i>	CCTGAATCCTGGACATTAGAAA	GGCTGGACAAGAGGGACTATG	270
<i>Cldn10</i>	GCTCTGTTATTGGATGGCA	ACAGATGTGGCCCATTGTA	125
<i>Cldn11</i>	TTTGGCTACTCCTGTATG	GAAC TGGAACCCGAAGAG	134
<i>Cldn12</i>	CTGAGTAGGGCTGTGAATACG	GCCAAGTGTCTGGTCAATAGT	310
<i>Ocln</i>	GAGCAGCAAAGGGATTCT	TCACACCCAGGATAGCAC	150
<i>Tjp1</i>	GGAGCATTGAAAGAAGCA	TGACAGGTAGGACAGACGA	123
<i>Actb</i>	GC GGG ACAT CAAGGAGAAC	AGCACCGTGTGGCGTAGAG	270
<i>Homo sapiens</i> (human)			
<i>Cldn1</i>	GCAGAAGATGAGGATGGCTGT	CCTTGGTGTGGTAAGAGGT	253
<i>Cldn2</i>	GCCATGATGGTGA CATCCAGT	TCAGGCACCAGTGGTAGTAG	218
<i>Cldn3</i>	GGACTTCTACAACCCGTGGT	AGACGTAGTCCTCGGGTCGT	230
<i>Cldn4</i>	CAAGGCCAAGACCATGATCGT	GCGGAGTAAGGCTGTCTGT	246
<i>Cldn5</i>	GGCACATGCA GTGCAAAGTGT	ATGTTGGCGAACAGCAGAGT	247
<i>Cldn6</i>	GGT GCTCACCTCTGGATTGT	GCAGGGCAGATGTTGAGTAG	267
<i>Cldn7</i>	CTCGAGCCATAATGGTGGTCT	CCCAGGACAGGAACAGGAGAG	326
<i>Cldn8</i>	CCGTGATGTCCTCTGGCTTC	CTCTGATGATGGCATTGGCAACC	176
<i>Cldn9</i>	GGTACACTGGCACCTGTGAT	GCTTCGACGGCTTAGAAC	312
<i>Cldn10</i>	CTGTGGAAAGCGTGC GCGTA	CAAAGAAGCCCAGGCTGACA	132
<i>Cldn11</i>	CTGATGATTGCTGCCTCGGT	ACCAATCCAGCCTGCATACAG	243
<i>Cldn12</i>	AGTCACTGCTCCGTCATACC	TTCTGAATCTGGCCCAAGTCT	250
<i>Ocln</i>	CTTCGCCTGTGGATGACTTC	CTTGCTCTGTTCTTTGACCT	117
<i>Tjp1</i>	CCTCAGCTGTGGAAGAGGATG	AGCTCCACAGGCTCAGGAAC	287
<i>Actb</i>	CTACCTCATGAAGATCCTACCGA	TTCTCTTAATGTACGCACGATT	84
<i>Mus musculus</i> (mouse)			
<i>Cldn1</i>	CCATGGCCAACGCGGGCTGC	TCACACATAGTCTTCCCAC	636
<i>Cldn2</i>	CCATGGCCTCCCTTGGCGTCC	CACACATAACCCAGTCAGGCTG	693
<i>Cldn3</i>	CATATGTCCATGGGTGG	TCAGACGTAGTCCTCGGGT	657
<i>Cldn4</i>	CCATGGCGTCTATGGGACTAC	TTACACATAGTTGCTGGCGG	633
<i>Cldn5</i>	CCATGGGTCTGCAGCGTTGG	GGCGAACAGCAGAGCGCAC	420
<i>Cldn6</i>	CCATGGCCTCTACTGGTCTGC	TCACACATAATTCTGGTGG	660
<i>Cldn7</i>	CCATGGCCAACCTGGGCTGCAAC	TCACACGTATTCTGGAGG	689
<i>Cldn8</i>	CCATGGCAACCTACGCTCTTC	CTACACATACTGACTTTGG	678
<i>Cldn9</i>	CCATGGCTTCACTGGCTTG	TCACACATAGTCCTCTTATC	654
<i>Cldn10</i>	CCATGGTAGCACGGCTTG	TTAGACATAGGCTTTTATC	696
<i>Cldn11</i>	CCATGGTAGGCCACTTGCCTC	TTAGACATGGCACTCTTG	624
<i>Cldn12</i>	CCATGGGCTGCCAGATGTCC	TTAAGTGTGTGAGACTAC	735
<i>Ocln</i>	CCATTTCTCGGGTTTCA	CTTCTGGATCTATGTACGGCTCA	207
<i>Tjp1</i>	GTAAAGCCTGGTGGTGGAACT	TCGAACCTCTACTCTACGACATG	174
<i>Actb</i>	CACAGCTGAGAGGGAAATC	TCAGCAATGCCCTGGTAC	336

*ACTB*, β-actin; *Cldn*, claudin; *Ocln*, occludin; *Tjp1*, tight junction protein 1 (alias for zonula occludin-1).

#### Reverse transcription-polymerase chain reaction (RT-PCR)

Total RNA was isolated from homogenized gland tissue with Trizol (Invitrogen, Carlsbad, CA, USA) according to the manufacturer's instructions. cDNA was prepared from 2 µg of total RNA with a

RevertAid First Strand cDNA Synthesis Kit (Promega, Madison, WI, USA). The mRNA for specific TJ proteins was amplified using Taq DNA Polymerase (Tsingke, Beijing, China) with specific primers (Table 1). The primers for porcine and human TJ proteins were designed according to the mRNA sequence retrieved from GenBank, and those for mouse proteins were designed according to

Khairallah et al. (2014). A negative control without an RNA template was included. The amplification products were visualized on a 1.5% agarose gel with ethidium bromide. The PCR products were confirmed by DNA sequencing.

## Results

### Morphological differences in the epithelial cells from different salivary glands

Salivary gland acinar cells can be classified as serous, mucous and seromucous cells according to their different polysaccharides contents, which can be discriminated by Alcian blue/periodic acid Schiff (AB/PAS) staining (Shackelford & Klapper, 1962). We identified the types of acinar cells from the porcine major salivary glands and compared the porcine SMG histological features with those of human and mouse SMGs, since most of the resting saliva in the oral cavity was produced by the SMG. The results showed that the porcine PG was composed purely of serous acinar secretory end pieces, which were PAS-positive and AB-negative (Fig. 1A). Both the porcine SMG and SLG were mixed glands containing serous cells (PAS-positive and AB-negative) and mucous cells (PAS-positive and strongly stained by AB). In the mixed acini, the serous cells were attached to the mucous secretory end pieces and formed a demilune, which was similar to that in human SMG (Fig. 1B–D). Although serous cells dominate the acinar cells in porcine and human SMGs, the human SMG contained more serous acinar cells ( $96.1 \pm 0.9\%$ ) compared with the porcine SMG ( $62.1 \pm 1.0\%$ ,  $P < 0.001$ ), as indicated by the AB/PAS staining. Differently, the murine acini of the SMG were composed of seromucous cells, which were moderately stained by AB (Fig. 1E). The main type of acinar cells in the porcine SLG was mucous cells, as  $62.8 \pm 1.4\%$  of the acinar cells had strongly positive AB staining (Fig. 1C).

The duct system of the porcine SMG was composed of intercalated, striated and excretory ducts containing no secretory granules, similar to the human SMG (Fig. 1B,D). However, the granular convoluted tubule predominated the duct system in the murine SMG, which was mainly composed of serous-like exocrine cells and contained abundant secretory granules that were PAS-positive (Fig. 1E).

The ultrastructural features of the porcine SMG showed that the serous acinar cells were loaded with secretory granules of high electron density, similar to the human SMG (Fig. 2A–C), and that the mucous acinar cells contained granules of low electron density (Fig. 2D,E). The murine acinar cells contained granules of low electron density (Fig. 2F). The ductal cells of the porcine and human SMGs showed similar characteristics to a centrally located nucleus and abundant mitochondria (Fig. 2G,H). However, specifically in the murine SMG, secretory granules of high electron density were gathered at the apical portion of the granular convoluted tubule cells (Fig. 2I).

### Comparisons of the expression pattern of TJ proteins in salivary glands among species

We screened the expression of claudin-1 to claudin-12, occludin and ZO-1 in the major salivary glands of pigs and compared them with those in human and mouse SMGs by RT-PCR. The results showed that all these TJ proteins were expressed in the porcine PG, SMG and SLG, and in the human SMG (Fig. 3). However, claudin-6, claudin-9 and claudin-11 were not detected in the murine SMG (Fig. 3).

The expression and distribution pattern of some representative TJ proteins in the SMGs of these three species are shown in Fig. 4. Immunofluorescence images showed that claudin-1, claudin-3 and claudin-4 immunostained positive in serous and mucous acinar cells and shared a similar distribution pattern in both porcine and human SMGs. These claudins were located in the cell membrane in the serous cells, whereas claudin-3 seemed to accumulate more in the apical-lateral membrane. Different from serous cells, these claudins were restrictively expressed in the apical-lateral membrane in the mucous cells. In the murine SMG, claudin-1 and claudin-3 were mainly present in the apical-lateral and basolateral membranes of acinar cells, whereas claudin-4 was only faintly stained in the apical-lateral area because the murine acinar cells were seromucous cells, a different cell type from pig and human acinar cells. Claudin-7 was not detected in the acini in the porcine SMG but was expressed in the lateral and basal membranes of acinar cells in the human and murine SMGs. Next, in the duct cells of human and porcine SMGs, claudin-1, claudin-4 and claudin-7 were widely expressed in the lateral and basal membranes and extended to the basal infoldings of ductal cells, whereas claudin-3 was mainly expressed in the apical-lateral area. However, in the murine SMG, claudin-1 and claudin-3 were weakly stained in the duct system. Claudin-4 was expressed in the apical-lateral membrane, whereas claudin-7 was located in the lateral and basal membranes of ductal cells; this staining was more intense than that in the acini. Occludin and ZO-1 displayed a conserved distribution pattern in these three species, as they were expressed in the apical-lateral membrane in both acinar and ductal cells.

To obtain a more comprehensive view of the TJ protein distribution, we recreated 3D images of the porcine SMG (Fig. 5). Although the 2D images showed that claudin-1, claudin-3 and claudin-4 were distributed in the apical-lateral membrane of the mucous acinar cells and the whole cell membrane of the serous acinar cells, 3D images showed that the intensity of the TJ proteins varied in different areas. The proteins were densely accumulated in the apical-lateral membranes and formed a group of continuous zig-zag lines in the lumina of acini. However, in the lateral and basal membranes where the TJ complex did not exist, these proteins were spread along the surface of the membrane with lower intensity (Fig. 5A). Claudin-1, claudin-4 and

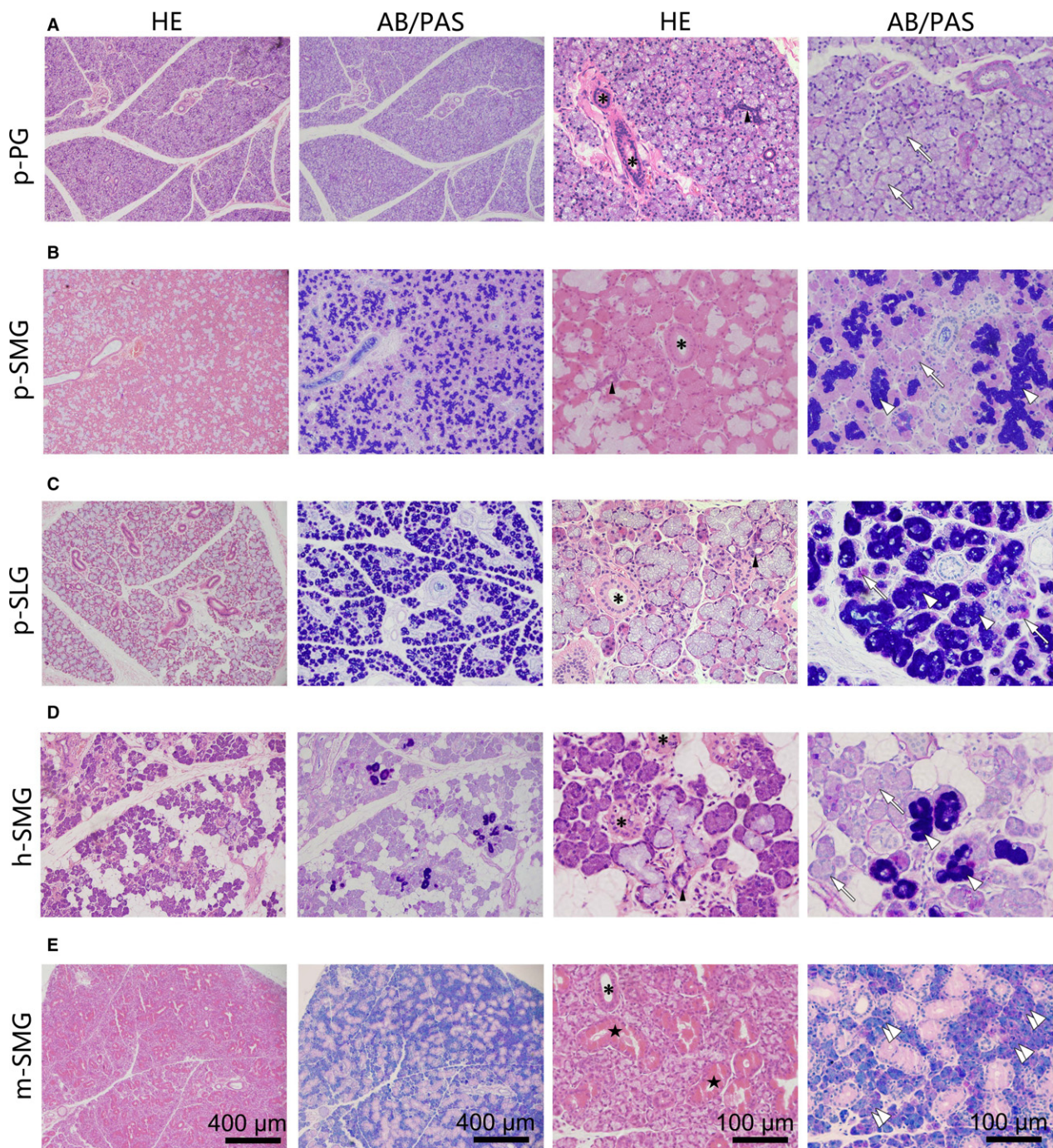


**Fig. 1** Comparisons of the major salivary glands examined by hematoxylin and eosin (H & E) staining and AB/PAS staining. (A) Porcine parotid gland. (B) Porcine submandibular gland. (C) Porcine sublingual gland. (D) Human submandibular gland. (E) Murine submandibular gland. The first and second rows are low-magnification micrographs, and the third and fourth rows are high-magnification micrographs. White arrow, serous acinus; white arrowhead, mucous acinus; double white arrowheads, seromucous acinus; black arrowhead, intercalated duct; asterisk, striated duct; pentagram, granular convoluted tubule. Scale bars: 400 µm in the first and second rows, 100 µm in the third and fourth rows.

claudin-7 were comparably expressed in both the lateral and basal membranes of ductal cells, whereas claudin-3 was expressed only in the apical lateral membrane (Fig. 5B). Occludin and ZO-1 were colocalized in the apical-lateral membrane of acinar and ductal cells (Fig. 5C,D). The

arrangement of TJ proteins that were expressed in the TJ complex of acini resembled an irregular polygon, whereas the proteins expressed on the luminal surface of ducts lined up and formed a honeycomb-like structure, with an orderly arrangement.

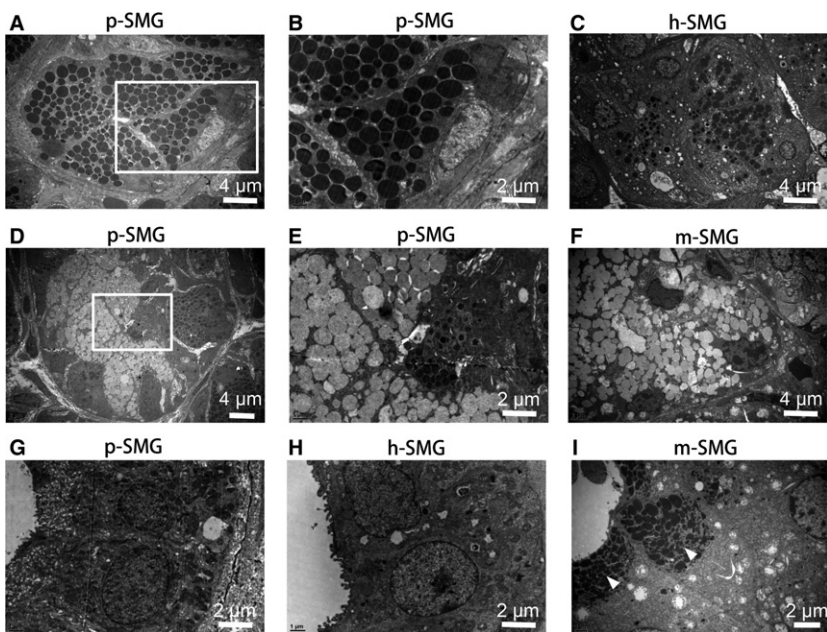


**Fig. 2** Comparisons of the ultrastructure of SMGs among species. (A–C) The serous acinus is composed of cells with high electron density granules in pig (A) and human (C). (B) Enlarged image from A. (D,E) The porcine mixed acinus is composed of serous cells with high electron density granules and mucous cells with low electron density granules. (E) Enlarged image from D. (F) Murine acinar cells containing granules of low electron density. (G,H) Striated duct cells of pig (G) and human (H). (I) Ductal cells of murine granular convoluted tubules containing high electron density (arrowheads) granules that are assembled in the apical portion. h, human; m, mouse; p, pig; SMG, submandibular gland.

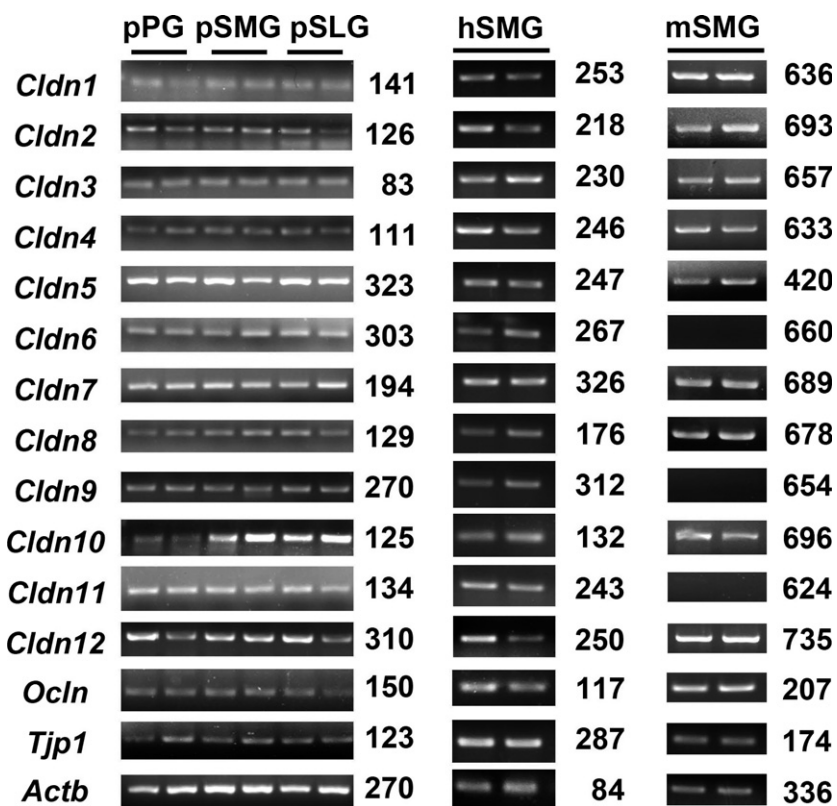


**Fig. 3** Expression of tight junction proteins in porcine major salivary glands and human and murine submandibular glands. Claudin-1 to claudin-12, occludin and zonula occludin-1 are detected in all three porcine major salivary glands and in human submandibular glands. Claudin-6, claudin-9 and claudin-11 are negative in the murine submandibular glands. Cldn, claudin; h, human; m, murine; Ocln, occludin; p, porcine; PG, parotid gland; SLG, sublingual gland; SMG, submandibular gland; Tjp1, tight junction protein 1 (zonula occludin-1).

## Discussion

Tight junction proteins play an important role in saliva formation through the paracellular pathway. Studies showed that the salivary gland dysfunction in SS and radiation-induced xerostomia is related to disruption of the TJ

structure (Ewert et al. 2010; Mellas et al. 2015; Nam et al. 2016; Zhang et al. 2016). The mechanism of how fluid and ions are transported through the paracellular pathway and the roles of TJs in the dysfunction of the salivary glands have not been fully clarified. Most of the studies on TJ proteins were carried out on rodents or cell lines derived from

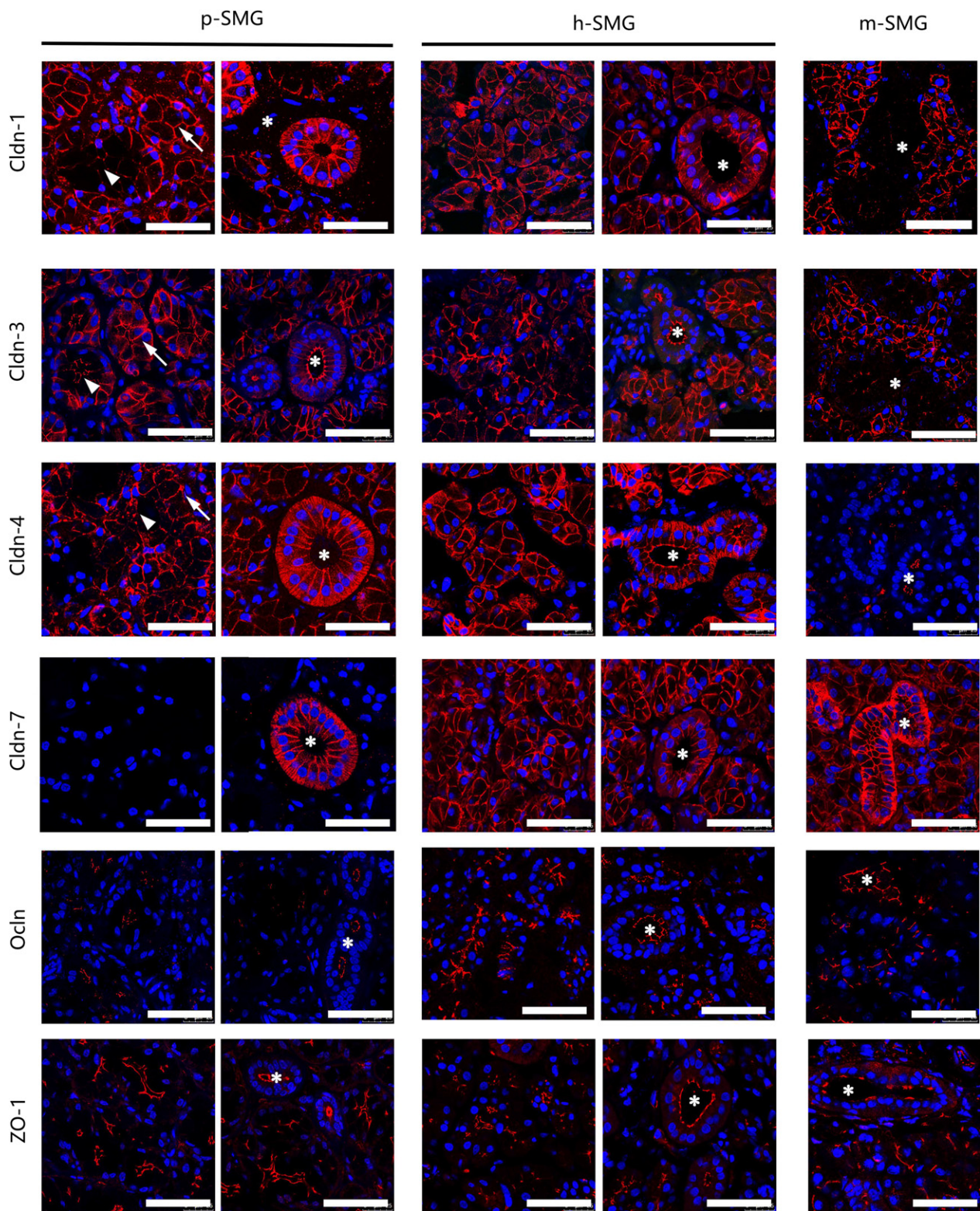


**Fig. 4** Comparisons of the distribution patterns of the tight junction proteins in submandibular glands (SMGs) among species. Claudin-1, claudin-3 and claudin-4 are detected in both acinar and ductal cells in porcine and human SMGs. Claudin-1 and claudin-3 are mainly located in acinar cells, whereas claudin-4 is predominantly expressed in ductal cells in mice. Claudin-7 is limited to the ductal cells in the porcine SMG but is detected in both acinar and ductal cells in the human and murine SMGs. Occludin and ZO-1 are expressed in the acinar and ductal cells in the three species. Cldn, claudin; h, human; m, murine; p, porcine; ZO-1, zonula occludin-1. Asterisk: Ducts; arrow, serous cells; arrowheads, mucous cells. Scale bars: 50 µm.

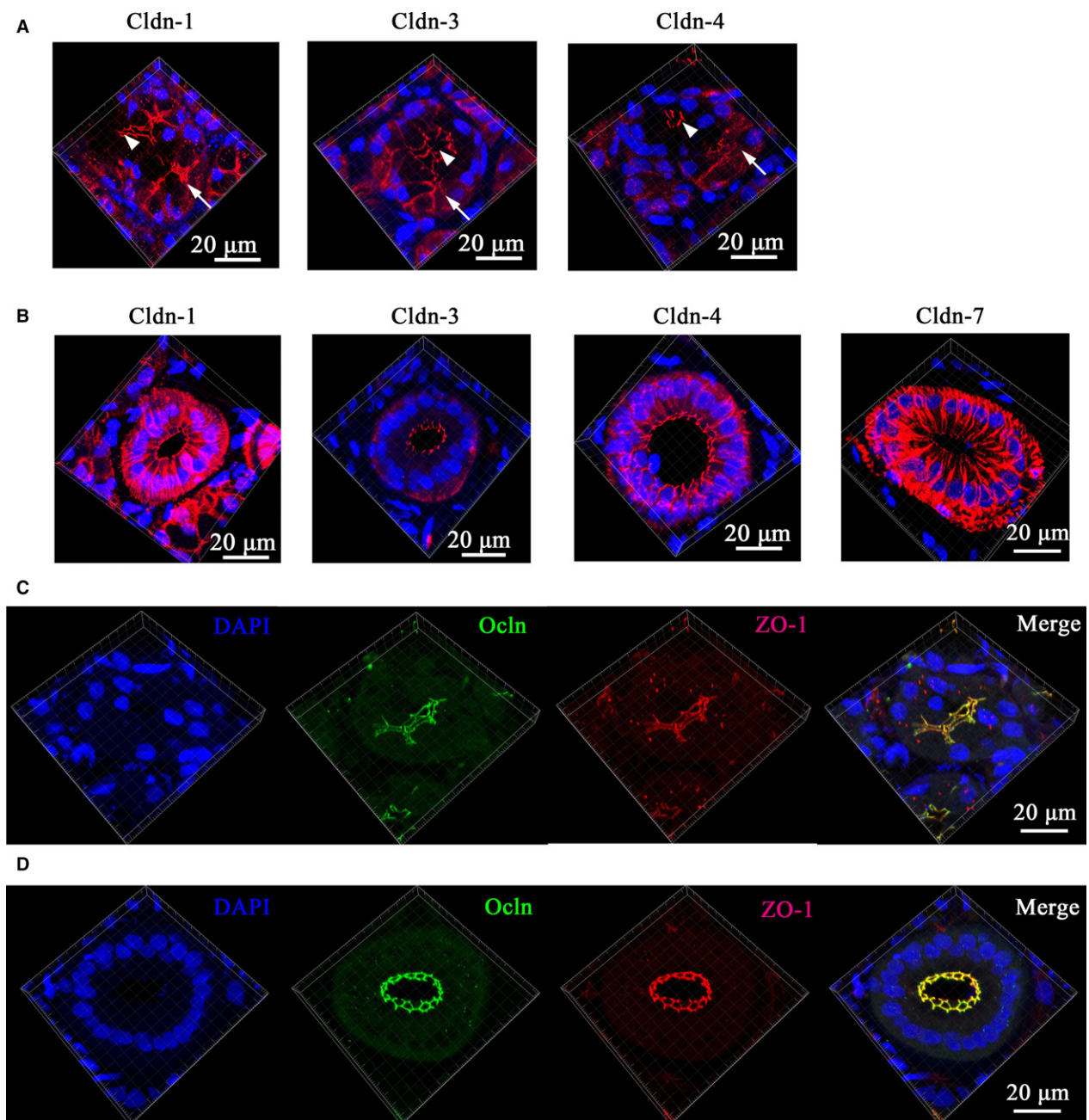


**Fig. 5** 3D images of the distribution of tight junction proteins in the porcine SMG. (A) Claudin-1, claudin-3 and claudin-4 are expressed in the apical-lateral membrane of mucous cells (arrowheads) and in both the apical and basal-lateral membranes of serous cells (arrows). (B) Claudin-3 is located in the apical-lateral membrane, whereas claudin-1, claudin-4 and claudin-7 are expressed in both the lateral membrane and the folds of basal membrane. (C) Occludin and ZO-1 are colocalized specifically in the apical-lateral membrane of the acinar cells. (D) Occludin and ZO-1 are colocalized in the apical-lateral membrane of the ductal cells. Cldn, claudin; Ocln, occludin; ZO-1, zonula occludin-1. Arrow, serous cells; arrowheads, mucous cells.

rats (Cong et al. 2013, 2015; Ding et al. 2013; Shi et al. 2014; Li et al. 2015; Mei et al. 2015; Mellas et al. 2015; Wang et al. 2016). However, the morphological and biochemical characteristics of salivary glands differ among species (Dreizen et al. 1968; Dowd et al. 1985; Dardick et al. 1990). Thus, it is important to identify an experimental

animal whose salivary glands are similar to those of humans. In the present study, we compared the histological features and the expression pattern of TJ proteins in porcine major salivary glands with those of human and murine SMGs; this comparison indicated that differences exist among species in TJ structure and function and that

miniature pigs are a candidate for studies on TJs in salivary glands.

The acinar cell types differ among different salivary glands and species. They are basically classified into three types according to the relative contents of neutral and acidic polysaccharides: (i) serous cells, which stain positive by PAS and negative by AB, contain various amounts of neutral polysaccharides but almost no acidic polysaccharides; (ii) mucous cells, which are PAS-positive and stained intensely with AB, contain large amounts of acidic polysaccharides but no neutral polysaccharides; and (iii) seromucous cells, which are also PAS-positive but react moderately with AB, and possess both carbohydrates (Shackleford & Klapper, 1962). Like those of humans, the porcine PGs were serous glands that exclusively secreted neutral polysaccharides and zymogen. The porcine SMGs and SLGs were mixed glands that secreted both neutral polysaccharides and acid mucous substances, although the porcine SMG contained more mucous cells than the human SMG. The duct system of porcine and human SMGs was well-developed with intercalated, striated and excretory ducts. However, the murine SMG was distinguished from that of human and pig in that, in the former, the acinar cell type was seromucous and the duct system contained the unique granular convoluted tubule.

The TJ protein expression pattern differed among species. Expression of claudin-1 to claudin-5, claudin-7 and claudin-16 was reported in human major salivary glands (Kriegs et al. 2007; Lourenco et al. 2007; Maria et al. 2008), and claudin-1, claudin-3 to claudin-8 and claudin-10 to claudin-12 are expressed in the murine embryonic SMG (Hashizume et al. 2004). However, there are few comprehensive studies on the expression of TJ proteins in human, porcine or adult murine salivary glands. Here, we found that claudin family members claudin-1 to claudin-12, occludin and ZO-1 were all expressed in the porcine major salivary glands and human SMG, whereas the adult murine SMG lacked the expression of claudin-6, claudin-9 and claudin-11. Notably, the expression of claudin family members in the adult murine SMG was slightly different from the embryonic SMG, in which claudin-6 and claudin-11 were detected, suggesting that claudin-6 and claudin-11 might be involved in SMG development. Next, we examined the location of some important TJ proteins, including claudin-1, claudin-3, claudin-4, claudin-7, occludin and ZO-1. Our results showed that claudin-1, claudin-3 and claudin-4 were present in serous mucous acinar cells and ductal cells in the porcine SMG and that the distributions were similar to those of humans. However, in the murine SMGs, the claudin-1 and claudin-3 staining was mainly distributed in acinar cell membranes, and claudin-4 was mainly distributed in the ducts, consistent with the findings reported by Zhang et al. (2016). Contradictions remained in the distribution pattern of claudin-1 in human salivary glands. Lourenco et al. (2007) reported that claudin-1 was present at the apical-lateral region of ductal

cells membranes but was not found in acinar cells, whereas Maria et al. (2008) found claudin-1 in 25% of serous acinar cells and ductal cells but not in mucous cells. Our results showed claudin-1 expression in both human acinar and ductal cells, similar to the expression in pigs. This discrepancy may be attributed to the different protocols used in different laboratories. Claudin-7 was limited in porcine ductal cells but was detected in both acinar and ductal cells in human and mouse, consistent with previous studies (Hashizume et al. 2004; Lourenco et al. 2007). Occludin and ZO-1 share the same distribution pattern among these species, with expression in the apical-lateral membrane of acinar and ductal cells.

The architecture of TJ proteins is shown in 3D images. In the luminal surface of the ducts, TJ proteins outlined the hexagon of each ductal cell and arranged to form a honeycomb-like structure, which is known to possess favorable mechanical properties such as high specific strength (Bae et al. 2011; Hedayati et al. 2016). In the acinar cells, the arrangement of TJ proteins was more irregular. This difference may be related to the different functions of the cells. Thus, 3D imaging of the TJ protein arrangement could be a valuable method of evaluating TJ function in future studies.

In summary, interspecies differences in the TJ protein expression of salivary glands should be taken into consideration when we draw conclusions from experimental results. Miniature pigs can be a candidate animal for studies on TJ structure and function in salivary glands.

## Acknowledgements

This study was supported by the Beijing Natural Science Foundation of China (No. 7172111) and the National Natural Science Foundation of China (Nos 81671005 and 81470756).

## Author contributions

Xue-Ming Zhang contributed to experiment performance, data acquisition, analysis and interpretation, and drafted the manuscript. Yan Huang, Kuo Zhang, Ling-Han Qu, Jia-Zeng Su and Xin Cong contributed to data acquisition. Li-Ling Wu, Yan Zhang and Guang-Yan Yu contributed to the conception and design of this study and critically revised the manuscript.

## References

- Amasheh S, Meiri N, Gitter AH, et al. (2002) Claudin-2 expression induces cation-selective channels in tight junctions of epithelial cells. *J Cell Sci* **115**, 4969–4976.
- Anderson JM (2001) Molecular structure of tight junctions and their role in epithelial transport. *News Physiol Sci* **16**, 126–130.
- Bae JH, Song HR, Kim HJ, et al. (2011) Discontinuous release of bone morphogenetic protein-2 loaded within interconnected pores of honeycomb-like polycaprolactone scaffold promotes

- bone healing in a large bone defect of rabbit ulna. *Tissue Eng Part A* **17**, 2389–2397.
- Cong X, Zhang Y, Yang NY, et al.** (2013) Occludin is required for TRPV1-modulated paracellular permeability in the submandibular gland. *J Cell Sci* **126**, 1109–1121.
- Cong X, Zhang Y, Li J, et al.** (2015) Claudin-4 is required for modulation of paracellular permeability by muscarinic acetylcholine receptor in epithelial cells. *J Cell Sci* **128**, 2271–2286.
- Dardick I, Naiberg J, Leung R, et al.** (1990) Ultrastructural study of acinar and intercalated duct organization of submandibular and parotid salivary gland. *Lab Invest* **63**, 394–404.
- Ding C, Li L, Su YC, et al.** (2013) Adiponectin increases secretion of rat submandibular gland via adiponectin receptors-mediated ampk signaling. *PLoS ONE* **8**, e63878.
- Dowd F, Cheung P, Warren J, et al.** (1985) Comparison of cyclic amp-dependent protein kinases from salivary glands of four species. *J Dent Res* **64**, 1199–1203.
- Dreizen S, Goodrich JS, Levy BM** (1968) Comparison of the salivary glands and salivary electrolytes in man and marmoset. *Arch Oral Biol* **13**, 229–237.
- Ewert P, Aguilera S, Allende C, et al.** (2010) Disruption of tight junction structure in salivary glands from Sjogren's syndrome patients is linked to proinflammatory cytokine exposure. *Arthritis Rheum* **62**, 1280–1289.
- NC3Rs Reporting Guidelines Working Group** (2010) Animal research: reporting *in vivo* experiments: the ARRIVE guidelines. *Exp Physiol* **95**, 842–844.
- Guo L, Gao R, Xu J, et al.** (2014) AdLTR2EF1 $\alpha$ -FGF2-mediated prevention of fractionated irradiation-induced salivary hypofunction in swine. *Gene Ther* **21**, 866–873.
- Hashizume A, Ueno T, Furuse M, et al.** (2004) Expression patterns of claudin family of tight junction membrane proteins in developing mouse submandibular gland. *Dev Dyn* **231**, 425–431.
- Hedayati R, Sadighi M, Mohammadi-Aghdam M, et al.** (2016) Mechanical properties of additively manufactured octagonal honeycombs. *Mater Sci Eng C Mater Biol Appl* **69**, 1307–1317.
- Khairallah H, El Andalousi J, Simard A, et al.** (2014) Claudin-7, -16, and -19 during mouse kidney development. *Tissue Barriers* **2**, e964547.
- Kriegs JO, Homann V, Kinne-Saffran E, et al.** (2007) Identification and subcellular localization of paracellin-1 (claudin-16) in human salivary glands. *Histochem Cell Biol* **128**, 45–53.
- Li J, Shan Z, Ou G, et al.** (2005) Structural and functional characteristics of irradiation damage to parotid glands in the miniature pig. *Int J Radiat Oncol Biol Phys* **62**, 1510–1516.
- Li J, Cong X, Zhang Y, et al.** (2015) Zo-1 and -2 are required for TRPV1-modulated paracellular permeability. *J Dent Res* **94**, 1748–1756.
- Loureiro SV, Coutinho-Camillo CM, Buim ME, et al.** (2007) Human salivary gland branching morphogenesis: morphological localization of claudins and its parallel relation with developmental stages revealed by expression of cytoskeleton and secretion markers. *Histochem Cell Biol* **128**, 361–369.
- Maria OM, Kim JW, Gerstenhaber JA, et al.** (2008) Distribution of tight junction proteins in adult human salivary glands. *J Histochem Cytochem* **56**, 1093–1098.
- Mei M, Xiang RL, Cong X, et al.** (2015) Claudin-3 is required for modulation of paracellular permeability by TNF- $\alpha$  through ERK1/2/slugs signaling axis in submandibular gland. *Cell Signal* **27**, 1915–1927.
- Mellas RE, Leigh NJ, Nelson JW, et al.** (2015) Zonula occludens-1, occludin and e-cadherin expression and organization in salivary glands with Sjogren's syndrome. *J Histochem Cytochem* **63**, 45–56.
- Mineta K, Yamamoto Y, Yamazaki Y, et al.** (2011) Predicted expansion of the claudin multigene family. *FEBS Lett* **585**, 606–612.
- Miyoshi J, Takai Y** (2005) Molecular perspective on tight-junction assembly and epithelial polarity. *Adv Drug Deliv Rev* **57**, 815–855.
- Miyoshi J, Takai Y** (2008) Structural and functional associations of apical junctions with cytoskeleton. *Biochim Biophys Acta* **1778**, 670–691.
- Muller D, Kausalya PJ, Claverie-Martin F, et al.** (2003) A novel claudin 16 mutation associated with childhood hypercalcemia abolishes binding to ZO-1 and results in lysosomal mistargeting. *Am J Hum Genet* **73**, 1293–1301.
- Nam K, Maruyama CL, Trump BG, et al.** (2016) Post-irradiated human submandibular glands display high collagen deposition, disorganized cell junctions, and an increased number of adipocytes. *J Histochem Cytochem* **64**, 343–352.
- Pedersen AM, Bardow A, Jensen SB, et al.** (2002) Saliva and gastrointestinal functions of taste, mastication, swallowing and digestion. *Oral Dis* **8**, 117–129.
- Shackleford JM, Klapper EC** (1962) Structure and carbohydrate histochemistry of mammalian salivary glands. *Am J Anat* **111**, 25–47.
- Shi L, Xiao M, Dai ML, et al.** (2014) Ischemia preconditioning protects rat submandibular glands from ischemia/reperfusion injuries. *Eur J Oral Sci* **122**, 324–331.
- Simon DB, Lu Y, Choate KA, et al.** (1999) Paracellin-1, a renal tight junction protein required for paracellular Mg<sup>2+</sup> resorption. *Science* **285**, 103–106.
- Van Itallie C, Rahner C, Anderson JM** (2001) Regulated expression of claudin-4 decreases paracellular conductance through a selective decrease in sodium permeability. *J Clin Invest* **107**, 1319–1327.
- Wang Z, Zourelias L, Wu C, et al.** (2015) Ultrasound-assisted nonviral gene transfer of AQP1 to the irradiated minipig parotid gland restores fluid secretion. *Gene Ther* **22**, 739–749.
- Wang CS, Wee Y, Yang CH, et al.** (2016) Alx/fpr2 modulates anti-inflammatory responses in mouse submandibular gland. *Sci Rep* **6**, 24244.
- Zhang LW, Cong X, Zhang Y, et al.** (2016) Interleukin-17 impairs salivary tight junction integrity in Sjogren's syndrome. *J Dent Res* **95**, 784–792.
- Zhou J, Wang H, Yang G, et al.** (2010) Histological and ultrastructural characterization of developing miniature pig salivary glands. *Anat Rec (Hoboken)* **293**, 1227–1239.
- Zhu Z, Pang B, Iglesias-Bartolome R, et al.** (2016) Prevention of irradiation-induced salivary hypofunction by rapamycin in swine parotid glands. *Oncotarget* **7**, 20271–20281.